Extra-Large-Pore Zeolites

DOI: 10.1002/anie.201001506

The Synthesis of an Extra-Large-Pore Zeolite with Double Three-Ring Building Units and a Low Framework Density**

*Jiuxing Jiang, Jose L. Jorda, Maria J. Diaz-Cabanas, Jihong Yu, and Avelino Corma**

Zeolites are crystalline inorganic solids formed by TO_4 tetrahedra (T = Si, P, Al, Ge, etc.) with a well-defined system of regular pores having diameters up to about 2 nm.[1,2] The possibility of tuning pore dimensions and framework compositions have made zeolites the most successful materials for applications in gas adsorption and separation and for catalysis.[3,4] Their uses have been further expanded[3] to microelectronics for preparing materials with low values of the high-frequency dielectric constant[5] or manufacturing encapsulated light-emitting devices (LEDs),[6] to medicine for diagnostic treatments[7] and controlled drug delivery, or for release of semiotics for controlling insect populations in agricultural uses.[8] Those applications often require structures with low framework densities, large internal volumes, and preferentially, extra-large pores. However, up to now, the number of known zeolites with a low framework density (FD $\leq$ 12) is almost negligible, and the number with extra-large pores ($\geq$ 18-R) is also extremely small.[1]

Computational methods can predict a large number of thermodynamically feasible new structures, and they can stimulate and inspire the discovery of new structures.[9–11] For example, Foster and Treacy[10] have used a symmetry-constrained intersite bond searching method and have generated more than two million structures. With that methodology, the authors predicted a series of thermodynamically feasible extra-large-pore zeolites. Deem et al.[11] have also modeled relatively large number of low density zeolites and were able to show that the low-energy and low-density materials also tend to have desirably large rings.

Among the zeolite structures with extra large pores predicted by Foster and Treacy, there is one with 18 × 10 × 10-R pore topology that could be of particular interest for catalysis, as it combines an extra-large pore (18-R) for molecular accessibility with connected 10-R pores that can introduce shape-selectivity effects. Recently, the predicted zeolite was synthesized and named ITQ-33.[12] This zeolite has 3-R and D4R units in the structure, and was at the time the silicate-based zeolite with the lowest framework density (12.3.T/1000 Å^3). The pore topology of this extra-large-pore zeolite presented quite unique and interesting catalytic properties: The pore accessibility to large molecules through the 18-R was combined with shape selectivity in the 10-R pores for the primary products formed.[13] In the same data base, Foster and Treacy also predicted an extra-large-pore zeolite that was closely related to ITQ-33 (Zeolite reference 191_4_1985). In that new structure, the 10-R pores of ITQ-33 were expanded to 12-R pores connecting the larger perpendicular 18-R channels. The result was a zeolite with 18 × 12 × 12 pore topology instead of the 18 × 10 × 10 for ITQ-33. In particular, along with D4R units, the new zeolite contains D3R units that have never been seen in synthesized zeolites, which could be related to geometric strains introduced in the framework owing to the formation of D3R based on silicon. In any case, the pore expansion with the 18 × 12 × 12-R pore system in the new zeolite should result in a decrease of the framework density from 12.3 in the case of ITQ-33 to 10.9 T atoms/1000 Å^3.

Herein, we show that the zeolite containing D3R that was predicted above can be successfully synthesized (ITQ-44) as a silicogermanate by combining a relatively inexpensive, rigid and bulky organic structure-directing agent (SDA) with the directing effect of germanium.[14] Furthermore, we show that in ITQ-44, germanium locates preferentially in D3R (with 50% Ge occupancy), followed by D4R (with 37% Ge occupancy).

ITQ-44 was synthesized using (2′-(*R*),6′-(*S*))-2′,6′-dimethylspiro[isoindole-2,1′-piperidin-1′-ium] as the SDA (Supporting Information, Figure S1). The synthesis of ITQ-44 was carried out in fluoride media using high-throughput (HT) synthesis techniques, which involve the use of a 15-well multiautoclave.

The XRD pattern of a calcined ITQ-44 sample (Figure 1) was collected (as described in the Supporting Information), and the crystal structure was solved using the program FOCUS.[16,17] The agreement between the observed and calculated XRD patterns are shown in Figure 1; it certainly confirms that this structure corresponds to that of the pure silica polymorph of this material predicted by Foster and Treacy[10] (reference number 191_4_19854).

The structure of ITQ-44 is closely related to the previously described zeolite ITQ-33 (Figure 2). It also comprises a building unit formed by a [$3^2 4^3 6^9$] cage with two additional

[*] J. Jiang, Dr. J. L. Jorda, Dr. M. J. Diaz-Cabanas, Prof. A. Corma
Instituto de Tecnologia Quimica (UPV-CSIC)
Universidad Politecnica de Valencia
Consejo Superior de Investigaciones Cientificas
Av. de los Naranjos s/n, 46022 Valencia (Spain)
Fax: (+34) 96-387-7809
E-mail: acorma@itq.upv.es
J. Jiang, Dr. J. Yu
State Key Laboratory of Inorganic Synthesis and Preparative Chemistry, College of Chemistry, Jilin University
Changchun 130012 (China)

[**] The authors thank the Spanish Government, Project CONSOLIDER-INGENIO 2010 and Generalitat Valenciana (Project Prometeo). J.J. thanks the China Scholarship Council for support and ITQ for a PhD scholarship.

Supporting information for this article is available on the WWW under http://dx.doi.org/10.1002/anie.201001506.

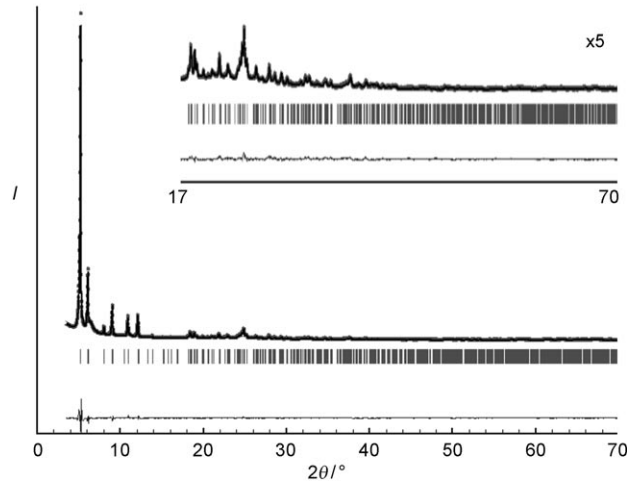

Figure 1. Rietveld refinement of the XRD pattern of ITQ-44 calcined at 823 K. Observed (●) and calculated (——) XRD patterns, along with the difference profile (bottom). The short tick marks below the pattern give the positions of the Bragg reflections. Inset: the pattern in the 2θ range 17–70° increased vertically by a factor of five.

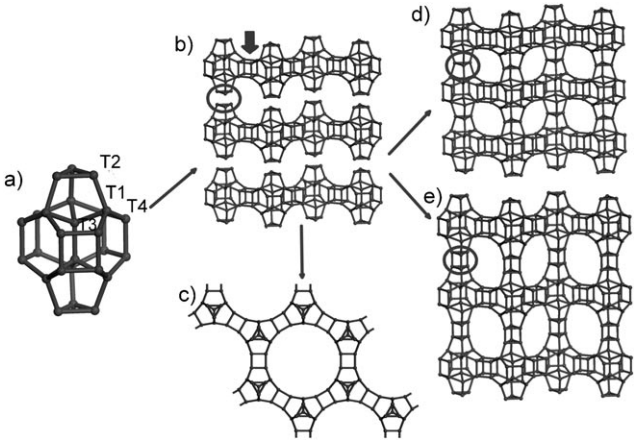

Figure 2. The structure of ITQ-44. a) Basic cluster of ITQ-44, indicating the location of the four independent T atoms. b) Connection of the basic units, forming D4R cages, as the origin of the basic sheets of the structure. The bold arrow indicates the connection. c) View of the structure along [001], showing the 18R channels. d) ITQ-33: Condensation of the basic sheets through the 3R, forming the 10R. e) ITQ-44: Connection of the 3R by bridging O atoms, forming the D3R and the 12R; the ellipses highlight the different connections in both zeolites. Oxygen atoms have been omitted for clarity.

atoms inside it, located along the direction of the *c* axis, which can be described as the clustering of three [$45^2 6^2$] and two [35^3] secondary building units sharing the T1–T3 edges (Figure 2a). In the case of zeolite ITQ-33 (Figure 2d), the tertiary building units give rise to the formation of columns along the *c* axis by sharing the three-membered ring (3R). For ITQ-44 however, the units are connected by bridging oxygen atoms between the 3Rs, giving rise to double three-ring units (D3R) corresponding to a [$3^2 4^3$] cage, which is a building unit previously unseen in synthesized zeolites (Figure 2e). As a consequence, the ten-membered-ring (10R) pores in ITQ-33 are expanded to 12R in ITQ-44 connecting the larger perpendicular 18R pores (Figure 2b–d). Furthermore, each column is linked to three neighboring columns through the four-membered rings, forming D4R cages. The ITQ-44 structure contains four symmetrically independent T-sites; the Rietveld refinement of the XRD pattern shows that the preferential isomorphic replacement of silicon atoms with germanium is, in general, comparable to that found in ITQ-33 with a similar chemical composition, but presents a noticeable difference, as will be described below. In the case of ITQ-44, the position T4 (corresponding to D4R) contains 37% Ge (compared with 39% Ge in ITQ-33), and T1 (position directly linked to the D4R) contains 26% Ge (33% in ITQ-33). The T3 site remains also as pure Si or (Si + Al) in both cases. However, there is a clear difference in the chemical composition of the T2 sites. In ITQ-33, this position corresponds to the 3R, and remains purely silicon (or as Si + Al). In ITQ-44 however, T2 sites conform to D3R, and they contain 50% Ge; that is, T2 becomes the most preferred position for the incorporation of germanium into the framework.

The chemical composition obtained from the Rietveld refinement is $[(Si+Al)_{0.66}Ge_{0.34}O_2]$, which closely matches that obtained by chemical analysis of the calcined sample ($H_{0.03}[Si_{0.65}Al_{0.03}Ge_{0.32}O_2]$). The topology of ITQ-44 presents a three-directional channel system, with straight extra-large channels with circular openings of 18 T atoms along the *c* axis direction (Figure 2c). This topology leads to a crystallographic pore diameter of 12.5 Å, similar to that found in ITQ-33 (12.2 Å), and a system of 12-ring channels in the plane *a*–*b*, with openings of 8.2×6.0 Å, which are larger than those in ITQ-33 (4.3×6.1 Å) that interconnect the 18-ring channels. The framework density (FD) of ITQ-44 is 10.9 T atoms per 1000 $Å^3$ (11.7 for the theoretical pure-silica form), which makes this structure the fully connected oxide-based zeolite with the lowest FD described to date. It is also has one of the lowest FD values for a zeolitic structure, together with the gallium–germanium sulfide UCR-20,[19] and the non-fully connected silicogermanate ITQ-37[2] and gallophosphate cloverite.[20] This value is well below those found in other zeolites containing 18-ring pores, such as ECR-34 (15.4),[21] VPI-5 (14.5),[22] or even ITQ-33 (12.3).[12]

It is known that fluoride has a tendency to occupy the center of small cages in zeolites.[23] In the case of ITQ-44, the ^{19}F MAS NMR spectrum of the as-synthesized zeolite (Supporting Information, Figure S4) has been related to the presence of fluoride anions in D4R cages. It appears then that in ITQ-44 the presence of fluoride ions in the D3R cages can be neglected.

The aluminum present in the zeolite is mostly tetrahedrally coordinated, as observed from the ^{27}Al MAS NMR spectrum (Supporting Information, Figure S5), suggesting that aluminum occupies zeolite framework positions. It should be noted that a small signal at 0–5 ppm is also observed, suggesting that in the as-synthesized sample there is a small amount of octahedrally coordinated aluminum, which must occupy extra framework positions.

In conclusion, a new extra-large zeolite (ITQ-44) has been synthesized with a $18 \times 12 \times 12$-R pore system that has the lowest framework density among the fully connected silica-based zeolites reported to date. The structure has a new

secondary building unit formed by a double three-membered-ring cage D3R that has previously not been observed in synthesized zeolites. There is a preferential germanium occupancy of the D3R.

This structure was theoretically predicted by Foster and Treacy, and shows the value of theoretical modeling for zeolite synthesis. In the case of germanium silicate zeolites, the presence of germanium is a handicap from an economical and the structure-stability point of view. In recent years, it has been shown that by choosing a more optimized organic structure-directing agent, it is possible to decrease or even completely remove the germanium in the synthesis process.[24,25] Very recently, Valtchev et al. have presented the possibility of carrying out isomorphic substitution of aluminum by germanium by a post-synthesis treatment.[26] These are encouraging results for transforming germanosilicates with interesting structures into the corresponding germanium-free materials.

Experimental Section

Synthesis of the structure-directing agent (SDA): (2′-(*R*), 6′-(*S*))-2′,6′-dimethylspiro[isoindole-2,1′-piperidin-1′-ium] was obtained in a one-step reaction. 1,2-Bis(bromomethyl)benzene and cis-2,6-dimethylpiperidine were combined in a 1:1 molar ratio in the presence of K_2CO_3 and heated under reflux for two days. The bromide was converted into the hydroxide (SDAOH) by ion exchange. Further details are given in the Supporting Information.

Synthesis of the zeolite: We started with an initial experimental factorial design ($3 \times 3 \times 5$; see the Supporting Information, Figure S2) in which Si/Ge, TIII/(Si+Ge), and F^-/(Si+Ge) were the synthesis variables. Crystallization temperature and time were fixed at 175 °C and one day. The optimum synthesis gel composition was $0.67\,SiO_2$:$0.33\,GeO_2$:$0.05\,Al_2O_3$:0.25 SDAOH:$0.20\,NH_4F$:$0.05\,NH_4Cl$:$2\,H_2O$. Further details are given in the Supporting Information.

The thermogravimetric analysis of the as-prepared ITQ-44 shows a total weight loss of 20 wt %, which corresponds to the organic SDA occluded within the zeolite. The chemical analysis of the sample indicates that the SDA is intact in the pores, with a C/N ratio of 14.2, which is close to the theoretical value of 15. (^{13}C and ^{29}Si MAS NMR spectra of the as-synthesized ITQ-44 are given in the Supporting Information, Figure S3.) ^{13}C MAS NMR spectra confirms the preservation of the template within the pores. Argon adsorption gave a peak centered at 1.0 nm with a shoulder at 0.75 nm. Nitrogen adsorption measurements gave a BET surface area of 470 $m^2 g^{-1}$, which could be underestimated owing to some loss of crystallinity during the calcination process.

Received: March 12, 2010
Published online: June 11, 2010

Keywords: high-throughput screening · microporous materials · structure elucidation · synthesis design · zeolites

[1] Ch. Baerlocher, L. B. McCusker, http://www.iza-structure.org/databases/.
[2] J. Sun, C. Bonneau, A. Cantín, A. Corma, M. J. Díaz-Cabañas, M. Moliner, D. Zhang, M. Li, X. Zou, *Nature* **2009**, *458*, 1154 – 1157.
[3] M. E. Davis, *Nature* **2002**, *417*, 813 – 821.
[4] A. Corma, *J. Catal.* **2003**, *216*, 298 – 312.
[5] Z. Li, M. C. Johnson, M. Sun, E. T. Ryan, D. J. Earl, W. Maichen, J. I. Martin, S. Li, C. M. Lew, J. Wang, M. W. Deem, M. E. Davis, Y. Yan, *Angew. Chem.* **2006**, *118*, 6477 – 6480; *Angew. Chem. Int. Ed.* **2006**, *45*, 6329 – 6332.
[6] P. Atienzar, M. J. Díaz-Cabañas, M. Moliner, E. Peris, A. Corma, H. García, *Chem. Eur. J.* **2007**, *13*, 8733 – 8738.
[7] S. W. Young, F. Qing, D. Rubin, K. J., Jr. Balkus, J. S. Engel, J. Lang, W. C. Dow, J. D. Mutch, R. A. Miller, *J. Magn. Reson. Imaging* **1995**, *5*, 499 – 508.
[8] J. Munoz-Pallares, E. Primo, J. Primo, A. Corma, *Stud. Surf. Sci. Catal.* **2001**, *135*, 5284 – 5288.
[9] M. E. Davis, *Nature* **1996**, *382*, 583 – 585.
[10] M. D. Foster, M. M. J. Treacy, http://www.hypotheticalzeolites.net/.
[11] M. W. Deem, R. Pophale, P. A. Cheeseman, D. J. Earl, *J. Phys. Chem. C* **2009**, *113*, 21353 – 21360.
[12] A. Corma, M. J. Diaz-Cabanas, J. L. Jorda, C. Martinez, M. Moliner, *Nature* **2006**, *443*, 842 – 845.
[13] M. Moliner, M. J. Diaz-Cabanas, V. Fornes, C. Martinez, A. Corma, *J. Catal.* **2008**, *254*, 101 – 109.
[14] A. Corma, M. T. Navarro, F. Rey, J. Rius, S. Valencia, *Angew. Chem.* **2001**, *113*, 2337 – 2340; *Angew. Chem. Int. Ed.* **2001**, *40*, 2277 – 2280.
[15] P. E. Werner, L. Eriksson, M. J. Westdahl, *Appl. Crystallogr.* **1985**, *18*, 367 – 370.
[16] Crystal data: hexagonal, *P6/mmm* (no.191), $a = 19.5358$ Å, $c = 14.4500$ Å, $V = 4776.0$ Å^3. Data collected as described in the Supporting Information. The cell was indexed using the program TREOR.[15] The crystal structure was solved using the program FOCUS.[17] Rietveld refinement was performed using the program FULLPROF,[18] with a visually estimated background and a pseudo Voight profile function. The conditions of the refinement are shown in the Supporting Information, Table S1. The residuals of the refinement were $R_{exp} = 0.029$, $R_{wp} = 0.109$, $R_F = 0.052$, $R_b = 0.038$. Rietveld refinements in lower-symmetry space groups did not produce an improvement in the refinement. Atomic coordinates, site occupancies, and thermal parameters of the refined structure are shown in the Supporting Information, Table S2. Further details on the crystal structure investigations may be obtained from the Fachinformationszentrum Karlsruhe, 76344 Eggenstein-Leopoldshafen, Germany (fax: (+49) 7247-808-666; e-mail: crysdata@fiz-karlsruhe.de), on quoting the depository number CSD-380436.
[17] R. W. Grosse-Kunstleve, L. B. McCusker, Ch. J. Baerlocher, *Appl. Crystallogr.* **1999**, *32*, 536 – 542.
[18] J. Rodríguez-Carvajal, *Commission on Powder Diffraction (IUCr) Newsletter* **2001**, *26*, 12 – 19.
[19] N. Zheng, X. Bu, P. Feng, *J. Am. Chem. Soc.* **2003**, *125*, 1138 – 1139.
[20] M. Estermann, L. B. McCusker, Ch. Baerlocher, A. Merrouche, H. Kessler, *Nature* **1991**, *352*, 320 – 323.
[21] K. G. Strohmaier, D. E. W. Vaughan, *J. Am. Chem. Soc.* **2003**, *125*, 16035 – 16039.
[22] M. E. Davis, C. Saldarriaga, C. Montes, J. Garces, C. Crowder, *Nature* **1988**, *331*, 698 – 699.
[23] A. W. Burton, S. I. Zones, S. Elomari, *Curr. Opin. Colloid Interface Sci.* **2005**, *10*, 211 – 219.
[24] A. Cantín, A. Corma, M. J. Diaz-Cabanas, J. L. Jorda, M. Moliner, *J. Am. Chem. Soc.* **2006**, *128*, 4216 – 4217.
[25] A. Cantín, A. Corma, M. J. Diaz-Cabanas, J. L. Jorda, M. Moliner, F. Rey, *Angew. Chem.* **2006**, *118*, 8181 – 8183; *Angew. Chem. Int. Ed.* **2006**, *45*, 8013 – 8015.
[26] F. Gao, M. Jaber, K. Bozhilov, A. Vicente, Ch. Fernandez, V. Valtchev, *J. Am. Chem. Soc.* **2009**, *131*, 16580 – 16586.

